

Sea Level and Thermal Response to the 1986-87 ENSO Event in the Far Western Pacific

John S. GODFREY, K. RIDGWAY, Gary MEYERS and Rick BAILEY

*CSIRO Division of Oceanography, GPO Box 1538,
Hobart, Tas. 7001, Australia*

ABSTRACT

Sea levels at the Papua New-Guinea (PNG) coast responded to the 1986-87 ENSO event much as would be expected for points on the inshore edge of a western boundary current, driven by remote sea level disturbances. The first EOF of sea level in the region accounts for 60% of the variance, and shows a clear western boundary current signal. Sea level estimates from tide gauges and adjacent XBT's are in good agreement, so XBT data are used to supplement sea level results; specifically, we obtain an estimate of the western boundary current as a function of depth. The anomalous transport varied by about 15 Sverdrups during the event. The boundary current followed the Tobriand Island ridge, rather than the main PNG coastline, and appears to bifurcate along southern New Britain. A maximum response to the ENSO occurred south of New Ireland, where steric sea level appeared to vary about 45 cm due to the ENSO event.

1. Introduction.

This report is a preliminary version of a comprehensive paper (Ridgway et al., in prep.). The 1986/87 ENSO event was the most completely monitored yet to have occurred. It is the first such event to occur in the TOGA decade and hence many new observing systems were in place. One such system (Fig.1) was a network of seven tide gauges installed around Papua New Guinea (PNG), which started operation in September 1984, enhancing the existing Pacific network (Wyrski, 1979). The density of the stations is greater than for elsewhere in the Pacific network, because it was anticipated that, along with observations of the large scale response to climatic variations, they might measure a western boundary current adjacent to the PNG mainland. During 1986-87, a weak ENSO event occurred (Miller et al., 1988). This provided the first opportunity to detect the presence or absence of these anomalous boundary currents and, if they were present in the sea level data, to obtain a picture of their behavior. It was hoped that the new network would provide answers to questions such as whether the western boundary current follows the PNG mainland coast (through Vitiaz Strait) or whether some or all of the anomalous transport follows along the coasts of New Britain and New Ireland.

2. Methods.

A full description of the instrumentation and procedures associated with the PNG sea level network is given in Ridgway (1989), hence only a brief discussion of the salient points will be included here. At each of the seven sites marked with solid squares in Fig.1, float-well gauges have been installed which incorporate Stevens analogue to digital recorders (ADR). The sea level data are recorded every 15 minutes on punched paper tape. A local observer collects the tape at the end of every month and sends the results to Hobart for processing.

XBT data covering the same time as the sea level data, for an area surrounding the expected western boundary currents, (outlined in Fig.1) were obtained from the TOGA Sub-surface Temperature Data Centre in Brest.



3. Data Processing.

The sea level data are processed in several stages in moving from the raw fifteen minute observations to a series of standard data products. Quality control procedures are used to remove any reference level and phase changes, and to fill small breaks in the data series. The observed series is then converted to hourly data using a simple binomial filter and a further Lanczos cosine filter is applied (Thompson, 1983) and the data are decimated to produce 12 hourly values. This removes the diurnal and semi-diurnal tidal frequencies but retains longer period signals, including those of tidal origin. In fact it was found that the fortnightly tides, Mf and Msf, were large enough to cause problems and so they were also removed. Plots of the time series of this 12 hourly data for all PNG stations are presented in Ridgway (1989).

Monthly mean sea levels were produced from simple averages of the hourly data. The annual cycle of sea level at each station was determined by procedures previously adopted by Wyrcki and Leslie (1980), in which a 2 harmonic curve was fitted to the data for the period September 1984 to December 1987. Monthly sea level anomalies were therefore obtained by subtracting the 1984-87 mean seasonal cycle of sea level from the monthly means. This procedure was also applied to the monthly mean data from other western Pacific stations (as published in the ISLPP maps (Wyrcki et al., 1988)).

Annual mean temperature-salinity relationships were obtained from the Levitus (1982) data set in $2^{\circ}\times 2^{\circ}$ squares, and used with the XBT's to obtain steric heights at the surface, and at 50, 100, 150, 200 and 300 db relative to 450 db. Individual steric height measurements were grouped into $2^{\circ}\times 2^{\circ}$ bins within the area show, in Fig. 1; 5 pairs of bins were combined, where data were thought to be inadequate in the individual bins.

4. Results.

a. Sea level

Fig.2 shows the monthly mean anomalies of sea level at the PNG gauges and several of the other western Pacific gauges. Most of the records show a drop in sea level towards the end of 1986, persisting for nearly 12 months; the magnitude and sharpness of the drop varies from station to station. The largest and sharpest drop occurs at Honiara where from December 1986 to April 1987 there was a 25 cm reduction in sea level. However, not all stations show this pattern; for example, there is no corresponding large negative anomaly in the sea level at Port Moresby, and anomalies in the monthly mean sea level there are restricted to about 5 cm over periods of 2 to 3 months.

An empirical Orthogonal Function (EOF) analysis was performed on the data from the 25 stations in the region for the period 1984 to 1987. This technique allow the most significant "standing wave" contributions to the variance to be extracted from each data record in the form of a set of orthogonal functions. Not surprisingly, the time amplitude of the first EOF (Fig. 3a) shows a drop at the end of 1986, as seen in many individual records in Fig.2; though for some reason the sharpness of this drop is greater than in most of the individual records. Nevertheless, this mode evidently captures the variance associated with the 1986-87 ENSO. The first mode accounts for 60% of the variance in sea level (the next mode only accounts for 16%). The corresponding spatial structure of the first EOF is show, in Fig. 4.

The large region of depressed sea level centred at Honiara seen in Fig. 4, within a generally zonal band between the equator and 15°S , is similar to behavior seen in earlier ENSO events (e.g. Wyrcki, 1985). The low sea level region is bounded by sharp gradients, implying strong westward and eastward geostrophic flow in the south and north respectively. A new feature, revealed by the PNG gauges, is that the westward flow is turned equatorward once having reached the PNG coast thus forming an anomalous western boundary current. Contours are hand drawn in Fig.4 , and it has been assumed that sea level

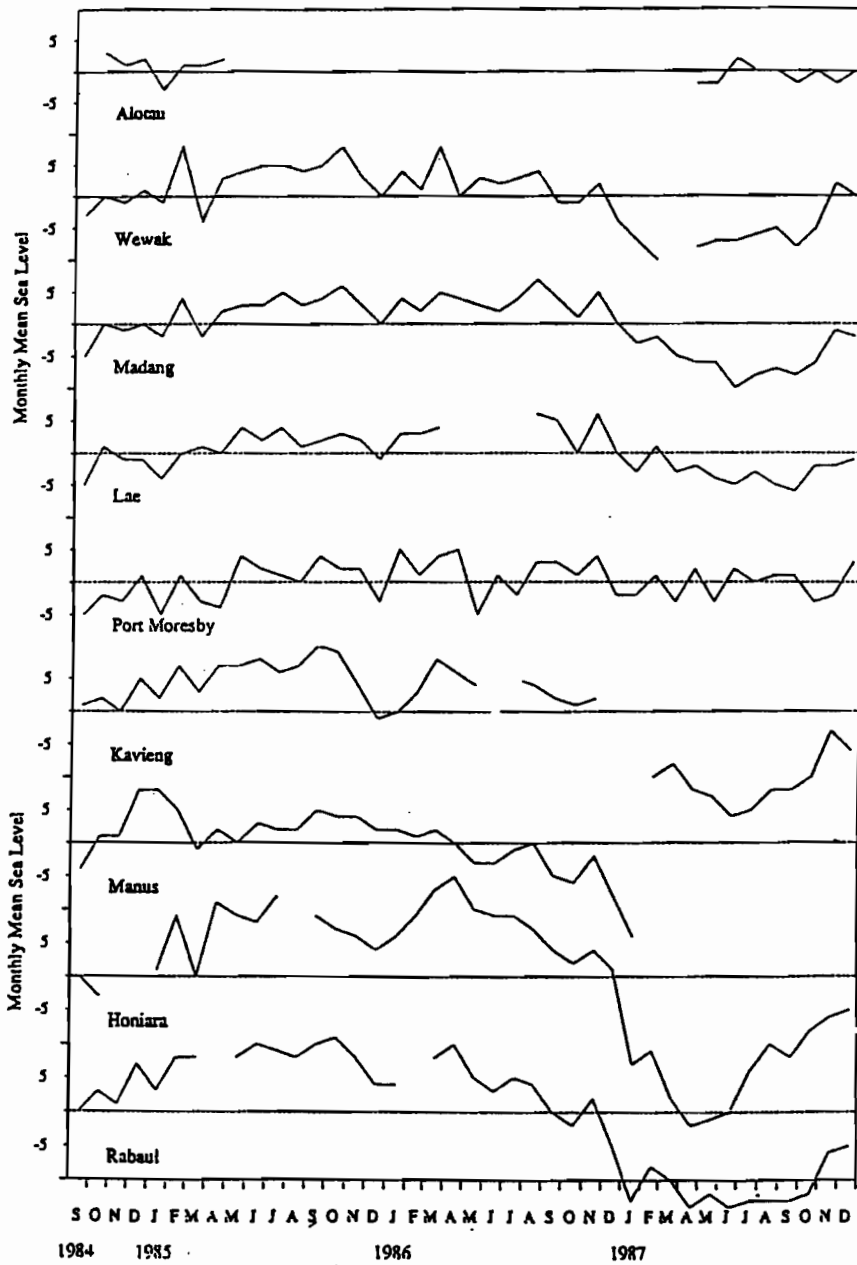


FIG.2. Monthly mean sea level anomalies at selected stations from Fig.1. Units along each ordinate are in cm.

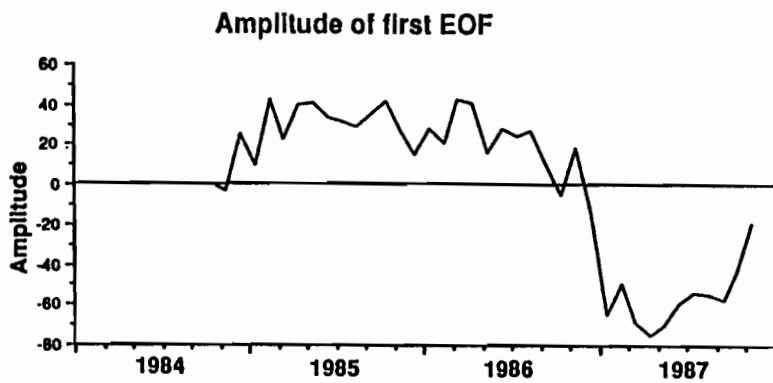


FIG.3. Time amplitude of the first empirical orthogonal eigenfunction of the sea level anomaly, for the 25 stations inside the large square of Fig.1.

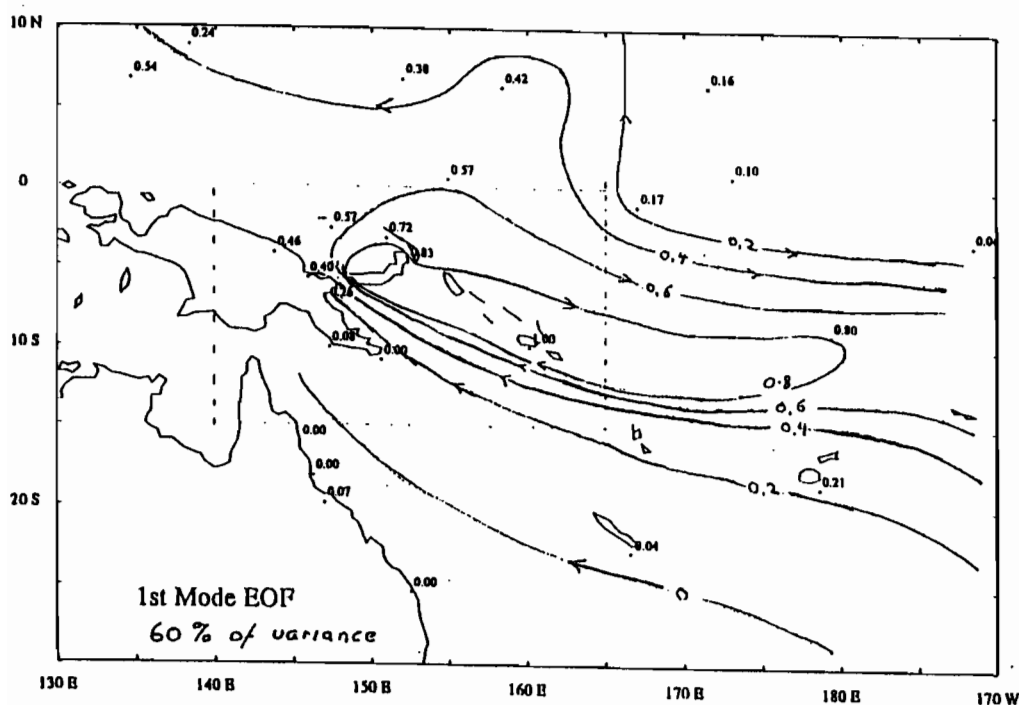


FIG.4. Spatial patterns of sea level anomaly in the first EOF of Fig.3. Contours have been hand-drawn, assuming that sea level is constant along the New Britain coast.

gradients along the New Britain coast are zero. Other choices, consistent with the observations, have non-zero gradients along the New Britain coast and less intense geostrophic currents through Vitiaz Strait; but a strong western boundary current remains.

It would be useful if some areas of ambiguity in this contour map of the sea level data could be removed. A sea level gauge at the western end of New Britain would be very useful for this purpose. Unfortunately data is not available on the western end of New Britain for the whole period; we do have, however, a limited data set spanning the 7-month period of the WEPOCS experiment (Lindstrom et al., 1987) for the stations Pililo, Long Island, Rabaul, Lae and Madang which encircle Vitiaz Strait. Plots of the band-pass filtered (tides and periods longer than 30 days removed) sea level have been prepared for each of these sites. As we are interested in the geostrophic current along the PNG coast we have used the Madang - Pililo and the Port Moresby - Honiara differences as representatives of this current. There is significant correlation for periods below 30 days and above the amplitude is at least of the same order; but the record is too short to resolve the contouring ambiguity in Fig.4.

b. Steric sea level.

A second approach is to augment the sea level data with results from XBT-derived steric heights. Before attempting this, it is useful first to compare XBT steric height observations taken within (say) 100 km of a tide gauge with the record of sea level from that gauge. Fig. 5 compares 12-hourly mean sea levels from tide gauges with simultaneous steric heights, from XBT's dropped within about 100 km of the gauge, for four representative stations. The difference between the two sets of observations has a standard deviation of less than ± 5 cm, even in the case of Lae where neither set of observations shows much variability. (Note that the seasonal signal has been retained in all the sets of observations in Fig. 5). These results confirm the general conclusion that XBT steric sea levels are a useful proxy for actual mean sea levels at islands (e.g. Rébert et al., 1985). In addition - rather surprisingly - Fig.5

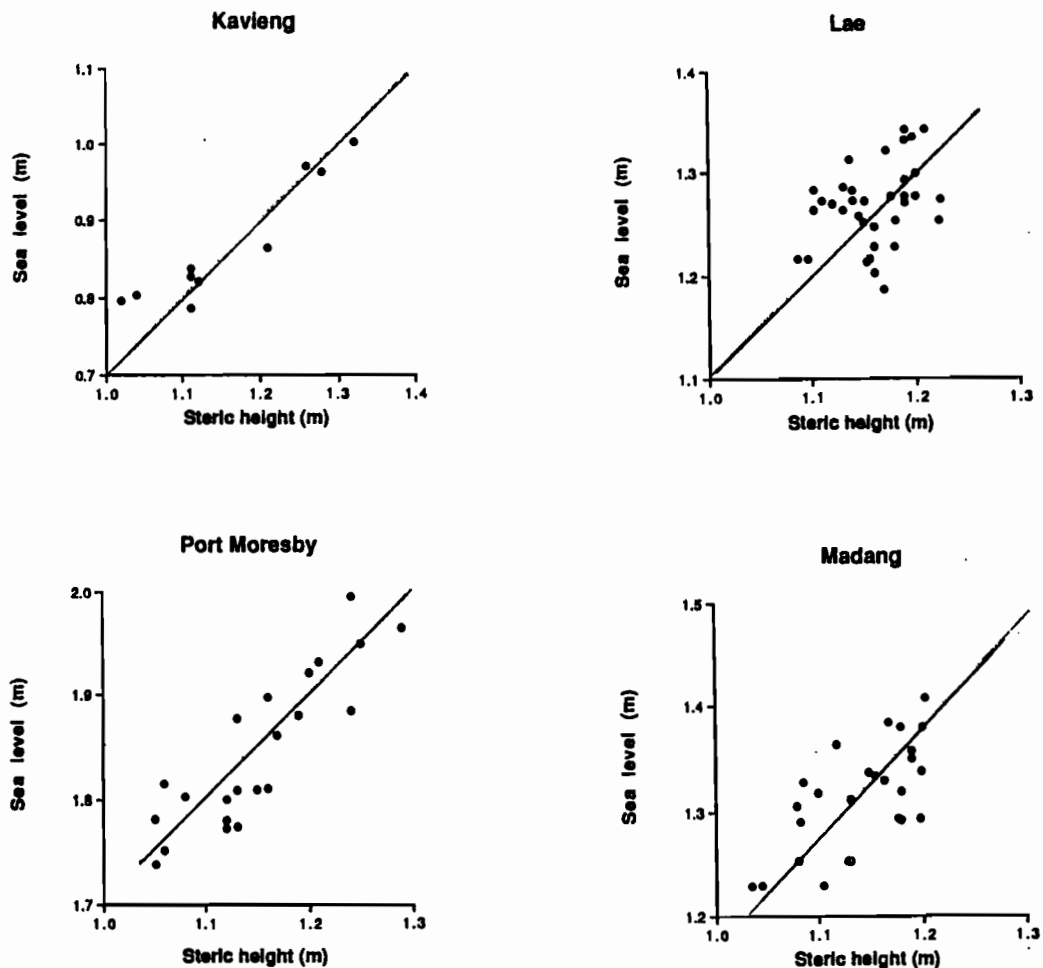


FIG.5. 12-hourly mean sea level at some coastal and island stations, compared to the simultaneous values of steric sea level within 100 km of the station (a) Kavieng, (b) Port Moresby, (c) Lae, (d) Madang.

suggests that this is true even for those of our gauges (Madang, Port Moresby, Lae) lying inshore from coastal boundary currents. This may simply reflect the fact that the continental shelf is narrow and the Coriolis parameter small for our gauge locations, so that geostrophic sea level differences between the tide gauge location and the shelf edge (where most of the XBT's are dropped) is likely to be small.

We have divided the region up into $2^{\circ} \times 2^{\circ}$ squares for further analysis, as illustrated in Fig.1. Fig.6 shows the time series of steric sea levels from a line of bins with centres along $153^{\circ}E$; the least-squares fit to these data by the first EOF amplitude of Fig.3 has been superimposed on each curve. Note that the amplitude of this curve (which is simply the regression coefficient of the time series of steric sea levels on the amplitude of the EOF) decreases suddenly between 7° and $9^{\circ}S$, and stays small at all points south of $9^{\circ}S$. Note also the very large amplitude of the best-fit curve at $7^{\circ}S$: this may be spurious, since no data are available in mid-1987 when the EOF amplitude of Fig.3 is very negative. Fig.7 shows the regression coefficients on the first EOF of Fig.3 from all $2^{\circ} \times 2^{\circ}$ squares, and from all sea level stations. Note that some $2^{\circ} \times 2^{\circ}$ squares have been combined, due to inadequate amounts of data in individual bins.

There are some substantial differences between Fig.7 and the original hand-contoured version of Fig.4, which was based on tide gauge data only. As already noted, the high

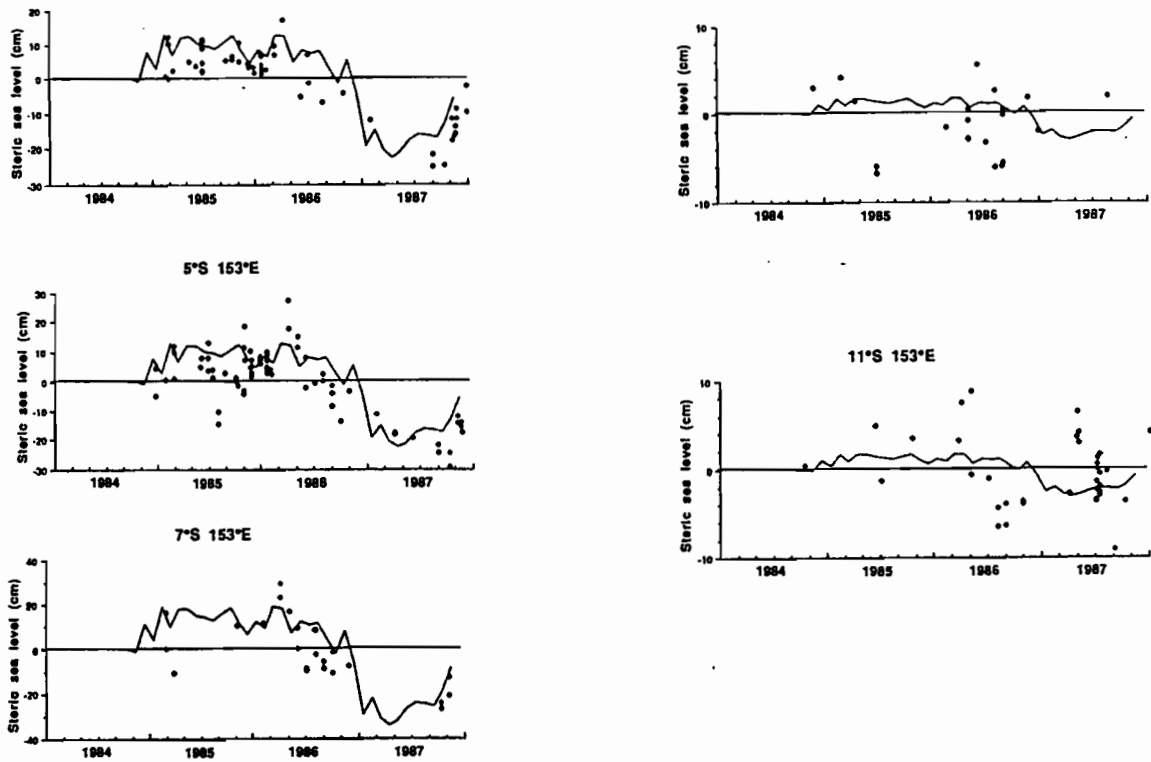


FIG.6. Time series of steric sea levels in $2^{\circ} \times 2^{\circ}$ bins, between 2° and 12° S, centred on 153° E. The time series of Fig.3, multiplied by its regression coefficient with the steric height data, is also shown. N.B. Seasonal cycle of steric height is still present in figure 6, but has been removed in preparing Fig.7. Note also the different vertical scales.

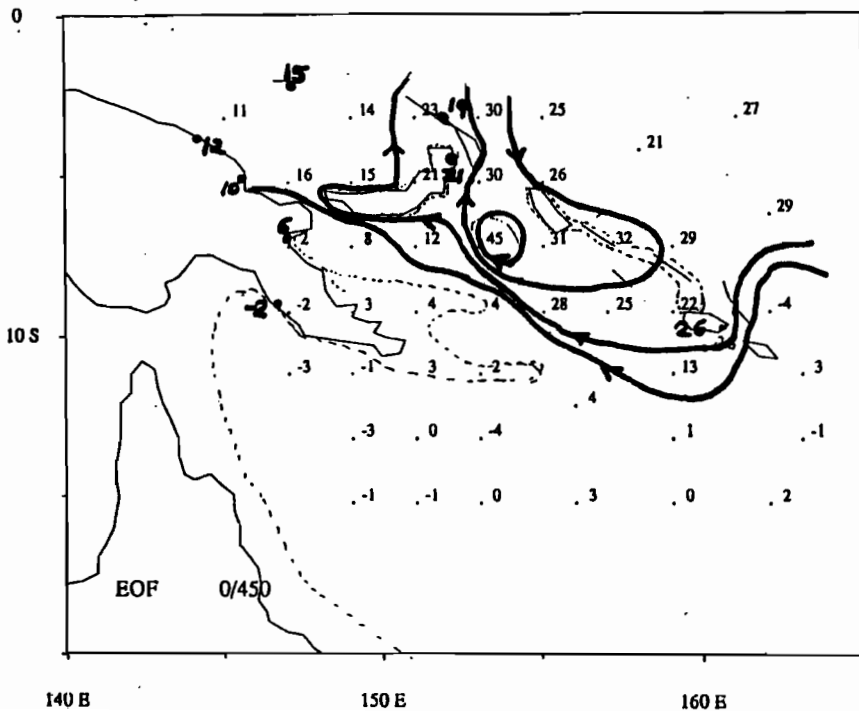


Fig.7. Contour plot of regression coefficients of steric height anomalies with the amplitude of Fig.3.

amplitude (45 cm) at (7°S, 153°E) may be due to a lack of data when the EOF was at a minimum, in this square. However, other differences between the two versions are probably real. In particular, there is a broad area off New Ireland and the northern Solomon islands where the regression coefficients are higher than found at any of the sea level gauges. It should be noted that the Solomons and Bougainville present a solid western boundary to the Pacific from 10°S to 5°S, below 200m, but there is a deep gap between northern Bougainville and New Ireland. Thus the higher values of ENSO response east of the Honiara and Rabaul gauges may reflect the Solomon island western boundary current.

Between 8° and 10°S, the PNG current is centred at 155°E in Fig.7. This result, though at first sight surprising, can be understood from PNG topography in these latitudes; the 200m contour extends to 153.5°E at 9°S (Budibudi Island). However, no such explanation can be offered for the fact that Fig.7 does *not* appear to show a western boundary current along the PNG coast between 6° and 8°S: the main geostrophic current appears to be some 400 km from the coast, i.e. near 153°E, and the water between 153°E and the PNG mainland is deep and unobstructed.

A strong "spike" is seen in several of the time series of steric heights, around April-May 1986 (e.g. Fig.6). This is partly due to the fact that Fig.6 shows full steric sea level values, rather than anomalies, but the spikes are present in the anomaly records as well. The spikes are mainly seen in the steric height records with large amplitudes in Fig.7, and is not seen in sea level records; it may influence the regression coefficients of fig.7. However - although we have not yet attempted to obtain an objective measure of the errors in the regression coefficients of Fig.7 - we do not believe the errors are large enough to account for all of the 30 cm difference in steric sea level between 151° and 153°E along 7°S, seen in Fig.7. If one accepts this feature as real, one possible explanation is that the eddy at (7°S, 153°E) may represent an inertial overshoot of the Solomon-Bougainville western boundary current, as it passes through the Bougainville - New Ireland gap.

This places some uncertainty on the interpretation of the flows along the PNG coast as western boundary currents: nevertheless, our best interpretation is that about half the current flows along the southern New Ireland coast, and another half through Vitiaz Strait; the small sea level difference between Rabaul and Kavieng suggests that little flow passes through St. George's Channel. It is interesting that the captain of the "Nimos" (the vessel that drops many of the XBT's in the PNG region) reports (pers. comm.) that they frequently encounter westward currents along the western half of the south New Britain coast and eastward currents along the eastern half of that coast. This agrees qualitatively with the interpretation of Fig. 7.

It may be noted that, perhaps due to the large number of islands through this region, the GEOSAT altimeter product of Miller et al., (1988) does not yet cover the region. Thus our data remains, for the present, the only source of information on the western boundary current anomalies in the Papua New Guinea region.

c. Geostrophic mass transports.

Maps such as Fig.7 have been prepared for the 50, 100, 150, 200 and 300 m levels from the XBT data. Briefly, each map is qualitatively similar to Fig.7, and shows the expected weakening with depth. The anomalous currents seem to have an e-folding depth of about 150 m (if our choice of a 450 db reference level is justified). Fig.8 shows the anomalous transports as a function of time, estimated from the sea level differences between Port Moresby and Honiara (10°S) and between Madang and Rabaul (5°S). The anomalous transport changes by about $15 \cdot 10^6 \text{m}^3 \text{s}^{-1}$ between mid-1986 and early 1987. Fig.7 suggests that these estimates may be too small, because they are based on sea level differences from tide gauges: thus they do not take into account the large changes in steric sea level just to the east of the Solomons and New Ireland.

Acknowledgments. We are indebted to Prof . K. Wyrski and Dr. R. Lukas for tide and pressure gauge data; also to the PNG tide gauge operators and the officers and crew of M/V

"Nimos" for obtaining much of the data in this paper.

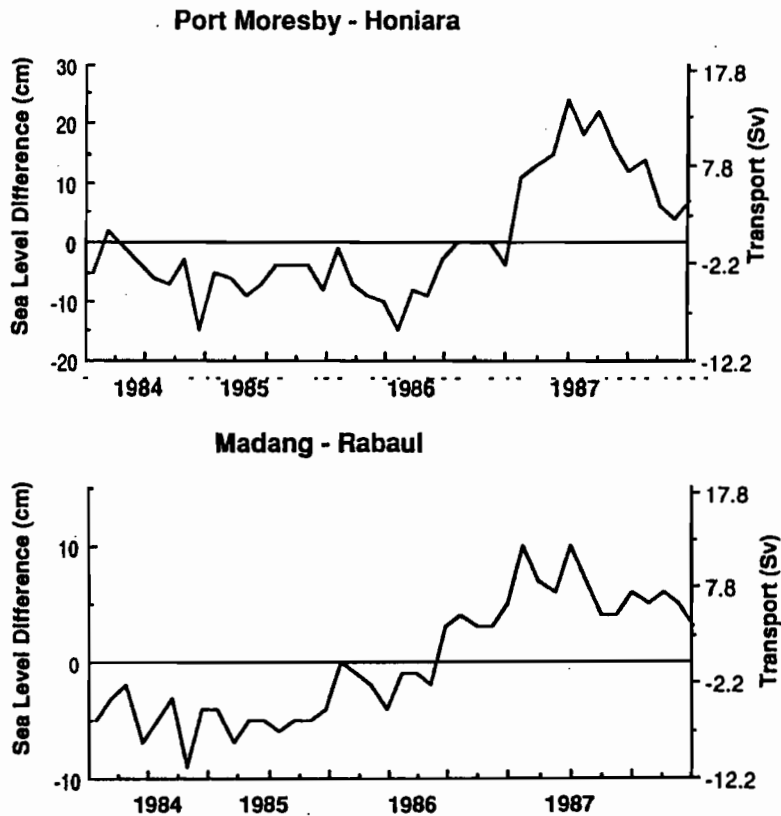


FIG.8. Amplitude of the geostrophic western boundary flow, estimated as the sea level differences $g(\text{Port Moresby-Honiara}) \times 150\text{m} / f(10^\circ\text{S})$; and as $(\text{Madang-Rabaul}) \times 150\text{m} / f(5^\circ\text{S})$.

REFERENCES

- Levitus, S., 1982: Climatological Atlas of the World Ocean. NOAA Professional Paper 13.
- Lindstrom, E., R. Lukas, R. Fine, E. Firing, J.S. Godfrey, G. Meyers, G., and M. Tsuchiya, 1987: The Western Equatorial Pacific Ocean Study. *Nature*, **330**, 533-537.
- Miller, L., R.E., Cheney and B.C., Douglas, 1988: GEOSAT altimeter observations of Kelvin waves and the 1986-87 El Nino. *Science*, **239**, 52-54.
- Rébert, J.D., J.R. Donguy, G. Eldin and K. Wyrtki, 1985: Relations between sea level, thermocline depth, heat content and dynamic height in the tropical Pacific Ocean. *J. Geophys. Res.*, **90**, 11, 719-11, 725.
- Ridgway, K.R. 1989: Sea level variations around Papua New Guinea; 1984-1987. CSIRO Marine Laboratories Report N° 73 pp.
- Thompson, R.O. R.Y., 1983: Low pass filters to suppress inertial and tidal frequencies. *J. Phys. Oceanogr.*, **13**, 1077-1083.
- Wyrtki, K., 1979: Sea level variations; Monitoring the breath of the Pacific. *Trans. Amer. Geophys. Union*, **60**, 25-27.
- Wyrtki, K., 1985: Sea level fluctuations in the Pacific during the 1982-83 El-Nino. *Geophys. Res. Lett.*, **12**, 125-128.
- Wyrtki K. and W. Leslie, 1980: The mean annual variations of sea level in the Pacific Ocean. University of Hawaii, HIG 80-5, 159 pages.
- Wyrtki, K., B. Kilonsky and S. Nakahara, 1988: The IGOSS Sea Level Pilot Project in the Pacific. JIMAR Contribution N° 88-°0150. Data Report N° 003.

**WESTERN PACIFIC INTERNATIONAL MEETING
AND WORKSHOP ON TOGA COARE**

Nouméa, New Caledonia

May 24-30, 1989

PROCEEDINGS

edited by

Joël Picaut *

Roger Lukas **

Thierry Delcroix *

* ORSTOM, Nouméa, New Caledonia

** JIMAR, University of Hawaii, U.S.A.

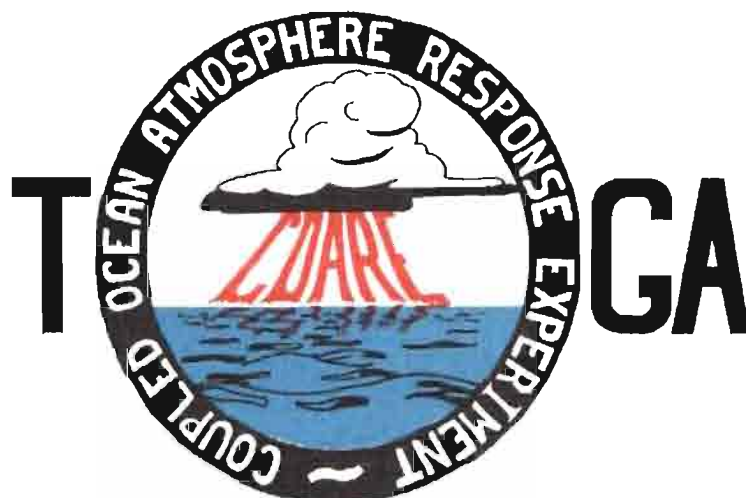


TABLE OF CONTENTS

ABSTRACT	i
RESUME	iii
ACKNOWLEDGMENTS	vi
INTRODUCTION	
1. Motivation	1
2. Structure	2
LIST OF PARTICIPANTS	5
AGENDA	7
WORKSHOP REPORT	
1. Introduction	19
2. Working group discussions, recommendations, and plans	20
a. Air-Sea Fluxes and Boundary Layer Processes	20
b. Regional Scale Atmospheric Circulation and Waves	24
c. Regional Scale Oceanic Circulation and Waves	30
3. Related programs	35
a. NASA Ocean Processes and Satellite Missions	35
b. Tropical Rainfall Measuring Mission	37
c. Typhoon Motion Program	39
d. World Ocean Circulation Experiment	39
4. Presentations on related technology	40
5. National reports	40
6. Meeting of the International Ad Hoc Committee on TOGA COARE	40
APPENDIX: WORKSHOP RELATED PAPERS	
Robert A. Weller and David S. Hosom: Improved Meteorological Measurements from Buoys and Ships for the World Ocean Circulation Experiment	45
Peter H. Hildebrand: Flux Measurement using Aircraft and Radars	57
Walter F. Dabberdt, Hale Cole, K. Gage, W. Ecklund and W.L. Smith: Determination of Boundary-Layer Fluxes with an Integrated Sounding System	81

MEETING COLLECTED PAPERS

WATER MASSES, SEA SURFACE TOPOGRAPHY, AND CIRCULATION

Klaus Wyrtki: Some Thoughts about the West Pacific Warm Pool	99
Jean René Donguy, Gary Meyers, and Eric Lindstrom: Comparison of the Results of two West Pacific Oceanographic Expeditions FOC (1971) and WEPOCS (1985-86)	111
Dunxin Hu, and Maochang Cui: The Western Boundary Current in the Far Western Pacific Ocean	123
Peter Hacker, Eric Firing, Roger Lukas, Philipp L. Richardson, and Curtis A. Collins: Observations of the Low-latitude Western Boundary Circulation in the Pacific during WEPOCS III	135
Stephen P. Murray, John Kindle, Dharma Arief, and Harley Hurlburt: Comparison of Observations and Numerical Model Results in the Indonesian Throughflow Region	145
Christian Henin: Thermohaline Structure Variability along 165°E in the Western Tropical Pacific Ocean (January 1984 - January 1989)	155
David J. Webb, and Brian A. King: Preliminary Results from Charles Darwin Cruise 34A in the Western Equatorial Pacific	165
Warren B. White, Nicholas Graham, and Chang-Kou Tai: Reflection of Annual Rossby Waves at The Maritime Western Boundary of the Tropical Pacific	173
William S. Kessler: Observations of Long Rossby Waves in the Northern Tropical Pacific	185
Eric Firing, and Jiang Songnian: Variable Currents in the Western Pacific Measured During the US/PRC Bilateral Air-Sea Interaction Program and WEPOCS	205
John S. Godfrey, and A. Weaver: Why are there Such Strong Steric Height Gradients off Western Australia ?	215
John M. Toole, R.C. Millard, Z. Wang, and S. Pu: Observations of the Pacific North Equatorial Current Bifurcation at the Philippine Coast	223

EL NINO/SOUTHERN OSCILLATION 1986-87

Gary Meyers, Rick Bailey, Eric Lindstrom, and Helen Phillips: Air/Sea Interaction in the Western Tropical Pacific Ocean during 1982/83 and 1986/87	229
Laury Miller, and Robert Cheney: GEOSAT Observations of Sea Level in the Tropical Pacific and Indian Oceans during the 1986-87 El Nino Event	247
Thierry Delcroix, Gérard Eldin, and Joël Picaut: GEOSAT Sea Level Anomalies in the Western Equatorial Pacific during the 1986-87 El Nino, Elucidated as Equatorial Kelvin and Rossby Waves	259
Gérard Eldin, and Thierry Delcroix: Vertical Thermal Structure Variability along 165°E during the 1986-87 ENSO Event	269
Michael J. McPhaden: On the Relationship between Winds and Upper Ocean Temperature Variability in the Western Equatorial Pacific	283

John S. Godfrey, K. Ridgway, Gary Meyers, and Rick Bailey: Sea Level and Thermal Response to the 1986-87 ENSO Event in the Far Western Pacific	291
Joël Picaut, Bruno Camusat, Thierry Delcroix, Michael J. McPhaden, and Antonio J. Busalacchi: Surface Equatorial Flow Anomalies in the Pacific Ocean during the 1986-87 ENSO using GEOSAT Altimeter Data	301

THEORETICAL AND MODELING STUDIES OF ENSO AND RELATED PROCESSES

Julian P. McCreary, Jr.: An Overview of Coupled Ocean-Atmosphere Models of El Nino and the Southern Oscillation	313
Kensuke Takeuchi: On Warm Rossby Waves and their Relations to ENSO Events	329
Yves du Penhoat, and Mark A. Cane: Effect of Low Latitude Western Boundary Gaps on the Reflection of Equatorial Motions	335
Harley Hurlburt, John Kindle, E. Joseph Metzger, and Alan Wallcraft: Results from a Global Ocean Model in the Western Tropical Pacific	343
John C. Kindle, Harley E. Hurlburt, and E. Joseph Metzger: On the Seasonal and Interannual Variability of the Pacific to Indian Ocean Throughflow	355
Antonio J. Busalacchi, Michael J. McPhaden, Joël Picaut, and Scott Springer: Uncertainties in Tropical Pacific Ocean Simulations: The Seasonal and Interannual Sea Level Response to Three Analyses of the Surface Wind Field	367
Stephen E. Zebiak: Intraseasonal Variability - A Critical Component of ENSO ?	379
Akimasa Sumi: Behavior of Convective Activity over the "Jovian-type" Aqua-Planet Experiments	389
Ka-Ming Lau: Dynamics of Multi-Scale Interactions Relevant to ENSO	397
Pecheng C. Chu and Roland W. Garwood, Jr.: Hydrological Effects on the Air-Ocean Coupled System	407
Sam F. Iacobellis, and Richard C.J. Somerville: A one Dimensional Coupled Air-Sea Model for Diagnostic Studies during TOGA-COARE	419
Allan J. Clarke: On the Reflection and Transmission of Low Frequency Energy at the Irregular Western Pacific Ocean Boundary - a Preliminary Report	423
Roland W. Garwood, Jr., Pecheng C. Chu, Peter Muller, and Niklas Schneider: Equatorial Entrainment Zone : the Diurnal Cycle	435
Peter R. Gent: A New Ocean GCM for Tropical Ocean and ENSO Studies	445
Wasito Hadi, and Nuraini: The Steady State Response of Indonesian Sea to a Steady Wind Field	451
Pedro Ripa: Instability Conditions and Energetics in the Equatorial Pacific	457
Lewis M. Rothstein: Mixed Layer Modelling in the Western Equatorial Pacific Ocean	465
Neville R. Smith: An Oceanic Subsurface Thermal Analysis Scheme with Objective Quality Control	475
Duane E. Stevens, Qi Hu, Graeme Stephens, and David Randall: The hydrological Cycle of the Intraseasonal Oscillation	485
Peter J. Webster, Hai-Ru Chang, and Chidong Zhang: Transmission Characteristics of the Dynamic Response to Episodic Forcing in the Warm Pool Regions of the Tropical Oceans	493

MOMENTUM, HEAT, AND MOISTURE FLUXES BETWEEN ATMOSPHERE AND OCEAN

W. Timothy Liu: An Overview of Bulk Parametrization and Remote Sensing of Latent Heat Flux in the Tropical Ocean	513
E. Frank Bradley, Peter A. Coppin, and John S. Godfrey: Measurements of Heat and Moisture Fluxes from the Western Tropical Pacific Ocean	523
Richard W. Reynolds, and Ants Leetmaa: Evaluation of NMC's Operational Surface Fluxes in the Tropical Pacific	535
Stanley P. Hayes, Michael J. McPhaden, John M. Wallace, and Joël Picaut: The Influence of Sea-Surface Temperature on Surface Wind in the Equatorial Pacific Ocean	543
T.D. Keenan, and Richard E. Carbone: A Preliminary Morphology of Precipitation Systems In Tropical Northern Australia	549
Phillip A. Arkin: Estimation of Large-Scale Oceanic Rainfall for TOGA	561
Catherine Gautier, and Robert Frouin: Surface Radiation Processes in the Tropical Pacific	571
Thierry Delcroix, and Christian Henin: Mechanisms of Subsurface Thermal Structure and Sea Surface Thermo-Haline Variabilities in the South Western Tropical Pacific during 1979-85 - A Preliminary Report	581
Greg. J. Holland, T.D. Keenan, and M.J. Manton: Observations from the Maritime Continent : Darwin, Australia	591
Roger Lukas: Observations of Air-Sea Interactions in the Western Pacific Warm Pool during WEPOCS	599
M. Nunez, and K. Michael: Satellite Derivation of Ocean-Atmosphere Heat Fluxes in a Tropical Environment	611

EMPIRICAL STUDIES OF ENSO AND SHORT-TERM CLIMATE VARIABILITY

Klaus M. Weickmann: Convection and Circulation Anomalies over the Oceanic Warm Pool during 1981-1982	623
Claire Perigaud: Instability Waves in the Tropical Pacific Observed with GEOSAT	637
Ryuichi Kawamura: Intraseasonal and Interannual Modes of Atmosphere-Ocean System Over the Tropical Western Pacific	649
David Gutzler, and Tamara M. Wood: Observed Structure of Convective Anomalies	659
Siri Jodha Khalsa: Remote Sensing of Atmospheric Thermodynamics in the Tropics	665
Bingrong Xu: Some Features of the Western Tropical Pacific: Surface Wind Field and its Influence on the Upper Ocean Thermal Structure	677
Bret A. Mullan: Influence of Southern Oscillation on New Zealand Weather	687
Kenneth S. Gage, Ben Basley, Warner Ecklund, D.A. Carter, and John R. McAfee: Wind Profiler Related Research in the Tropical Pacific	699
John Joseph Bates: Signature of a West Wind Convective Event in SSM/I Data	711
David S. Gutzler: Seasonal and Interannual Variability of the Madden-Julian Oscillation	723
Marie-Hélène Radenac: Fine Structure Variability in the Equatorial Western Pacific Ocean	735
George C. Reid, Kenneth S. Gage, and John R. McAfee: The Climatology of the Western Tropical Pacific: Analysis of the Radiosonde Data Base	741

Chung-Hsiung Sui, and Ka-Ming Lau: Multi-Scale Processes in the Equatorial Western Pacific	747
Stephen E. Zebiak: Diagnostic Studies of Pacific Surface Winds	757

MISCELLANEOUS

Rick J. Bailey, Helene E. Phillips, and Gary Meyers: Relevance to TOGA of Systematic XBT Errors	775
Jean Blanchot, Robert Le Borgne, Aubert Le Bouteiller, and Martine Rodier: ENSO Events and Consequences on Nutrient, Planktonic Biomass, and Production in the Western Tropical Pacific Ocean	785
Yves Dandonneau: Abnormal Bloom of Phytoplankton around 10°N in the Western Pacific during the 1982-83 ENSO	791
Cécile Dupouy: Sea Surface Chlorophyll Concentration in the South Western Tropical Pacific, as seen from NIMBUS Coastal Zone Color Scanner from 1979 to 1984 (New Caledonia and Vanuatu)	803
Michael Szabados, and Darren Wright: Field Evaluation of Real-Time XBT Systems	811
Pierre Rual: For a Better XBT Bathy-Message: Onboard Quality Control, plus a New Data Reduction Method	823